Thermochimica Acta 501 (2010) 8–12

Contents lists available at ScienceDirect

Thermochimica Acta

journal homepage: www.elsevier.com/locate/tca

Microcalorimetric and microscopic studies on the inhibitory activities of methylene blue/TiO_2 nanocomposites on *Staphylococcus aureus* and the mechanism of cell damage

Yue-Sheng Li[a,b], Yue Zhang[a], Ze-Zhong Chen[a], Ai-Qing Zhang[c], Hong-Wu Tang[a], Feng-Lei Jiang[a,*], Yi Liu[a]

[a] State Key Laboratory of Virology & Key Laboratory of Analytical Chemistry for Biology and Medicine (Ministry of Education) & College of Chemistry and Molecular Sciences, Wuhan University, Wuhan 430072, PR China
[b] Department of Chemistry and Life Sciences, Xianning University, Xianning 437005, PR China
[c] Key Laboratory of Catalysis and Materials Science of Hubei Province, South-Central Nationalities University, Wuhan 430074, PR China

ARTICLE INFO

Article history:
Received 19 October 2009
Received in revised form
16 December 2009
Accepted 27 December 2009
Available online 11 January 2010

Keywords:
Microcalorimetry
Staphylococcus aureus
MB/TiO_2 nanocomposites
Inhibitory activities
Thermokinetics

ABSTRACT

The effect of methylene blue/TiO_2 nanocomposites on *Staphylococcus aureus* was evaluated by a LKB-2277 Bioactivity Monitor at 37.0 °C. By analyzing the thermogenic power–time curves, kinetic parameters such as the growth rate constant (k), the maximum heat power of growth phase (P_m), generation time (t_G) and the inhibitory ratio (I) were determined. The k and P_m decrease while t_G and I increases with increasing concentrations of the methylene blue/TiO_2 nanocomposites added into the microbe suspension. Both k and I have linear correlations with the concentration of the methylene blue/TiO_2 nanocomposites. The effect of the methylene blue sensitized-TiO_2 nanocomposites on the cell damage of *S. aureus* was investigated by microscopic method.

1. Introduction

Microcalorimetry has been widely used in life sciences because of its high sensitivity, high accuracy and automaticity [1–4]. It has a great advantage on studies of complicated living systems, compared with the traditional microbiological techniques such as cell number counting and biomass which are considered to be time-consuming and less efficient, and provides a particularly useful tool for characterization of the microbial growth processes [5]. Besides, it is a nondestructive and noninvasive technique [6], so it can monitor various biological processes. From microcalorimetry the power–time curves of bacterial growth can be obtained. By analyzing the exponential growth phase of the power–time curves, kinetic parameters, the growth rate constant (k) for example, can be determined [7].

Methylene blue (methylenum caeruleum, tetramethylthionine chloride or swiss blue, MB, formula: $C_{16}H_{18}N_3ClS$; CAS registry number: 61-73-4) is a cationic dye with formal redox potential between 0.08 and −0.25 V (versus SCE) in solutions (pH 2–8) which is close to that of several biomolecules [8]. In 1960s, MB was tested for its photodynamic reaction with DNA [9]. Recently the interaction of MB with protein was studied by spectroscopic methods and the thermodynamic parameters were determined [10]. MB was also used as a photosensitizer for photosensitization of different *Candida* species [11]. Until now, MB has been widely used for electrochemical applications, for instance, as catalysts/mediators in electrochemical biosensors [8]. TiO_2 has been proved satisfactory sensitization with MB for photodegradation of various halocarbons using visible light [12]. Additionally, a mixture of commercial TiO_2 powder and MB has been used to fabricate an intelligent ink sensible to oxygen [13–16]. In addition, nanocrystalline TiO_2 catalyst was evaluated by measuring degradation rates of MB under UV or visible light. TiO_2 can be used for photodegradation of various pollutants due to its low cost, high photocatalytic activity and chemical stability [17,18]. Some of the work has focused on viruses [19,20], bacteria [21–23], yeast [24] and other types of cells [25,26]. For killing viruses, it is crucial to destroy their nucleic acids. Thus some researchers studied the ultraviolet light-induced photoox-

* Corresponding author at: State Key Laboratory of Virology & Key Laboratory of Analytical Chemistry for Biology and Medicine (Ministry of Education) & College of Chemistry and Molecular Sciences, Wuhan University, Wuhan 430072, P. R. China. Tel.: +86 27 68756667; fax: +86 27 68754067.
E-mail address: fljiang@gmail.com (F.-L. Jiang).

0040-6031/$ – see front matter © 2010 Elsevier B.V. All rights reserved.
doi:10.1016/j.tca.2009.12.015

idative damage to nucleic acids catalyzed by TiO_2 [27,28]. There are great interests in the interaction of bacteria with TiO_2, but the antibacterial behaviors of TiO_2 nanoparticle together with MB dye are still totally unclear until now. It is of great importance for the application of these bioconjugated nanomaterials, therefore a general analytical tool like microcalorimetry for studying the interaction of bacteria with nanomaterials is highly necessary to address the challenges of the arising field of nanobiotechnology [14–16].

In this paper, by using a LKB-2277 Bioactivity Monitor, the inhibitory effect of MB/TiO_2 nanocomposites on *Staphylococcus aureus* (*S. aureus*) at 37.0 °C was investigated to elucidate the effects of the MB/TiO_2 nanocomposites on biological process. Then the mechanism of cell damage of *S. aureus* was studied by transmission emission microscopy and Hadamard transform imaging microscopy. These studies can provide a comprehensive understanding of the effect of dyes-TiO_2 nanoparticle system on gram-positive bacteria.

2. Experimental

2.1. Materials

S. aureus (CCTCCAB910393) was provided by the Chinese Center for Type Culture Collections of Wuhan University (Wuhan, PR China). The broth culture medium (1000 mL) contained 5 g NaCl, 5 g beef extract (purchased from sigma) and 10 g peptone (purchased from sigma). The volume of each culture medium was 25 mL. The pH of medium was adjusted to 7.0–7.2 before autoclaving. It was sterilized in high pressure steam at 120 °C for 30 min. At the beginning of the experiments, *S. aureus* was inoculated in the peptone medium with a concentration of 2×10^6 cells mL^{-1}. The rotary speed of incubator shaker is 100 rpm. The flask is enveloped with cotton plug to supply enough oxygen for *S. aureus*. Then freshly prepared solutions of drugs (e.g. MB, TiO_2 and MB/TiO_2 nanocomposites) with different concentrations were added to the cell suspension.

The MB/TiO_2 nanocomposites suspension was prepared in PBS buffer solution (pH 7.4 ± 0.1) according to literature [15,16]. All solutions were prepared with doubly distilled water. Sample masses were accurately weighed on a microbalance (Sartorius, ME215S) with a resolution of 0.1 mg.

2.2. Equipments

A LKB-2277 bioactivity monitor (Thermometric AB, Sweden) was used to determine the metabolism of bacteria. The voltage signal was recorded by a computer. The baseline stability was 0.2 μW/24 h. The performance and structure of the instrument were given in detail elsewhere [2,6,7]. All calorimetric experiments were conducted at 37.0 °C. Hadamard transform imaging microscope system contain a cooled CCD (−10 °C) with a C7041 driving circuit and a C7557 controller (Hamamatsu, Japan), a research-grade fluorescence microscope (Chongqing Optic-Electro Instrument Company) and a monochromator (WDG-30, Beijing Optical Instrument Factory).

2.3. Experimental methods of microcalorimetry and Hadamard transform imaging microscope system

Stopped-flow method was used in this study. In all of the experiments, the flow cell was completely cleaned and sterilized in sequence by pumping sterilized distilled water, 0.1 mol L^{-1} of aqueous HCl, 75% alcohol solution, 0.1 mol L^{-1} of aqueous NaOH and sterilized distilled water assisted by a LKB-2132 microperpex peristaltic pump, each for 15 min at a flow rate of 50 mL h^{-1}. When a stable baseline was obtained, the cell suspension containing the bacteria and MB/TiO_2 nanocomposites was pumped into the flow cell at a flow rate of 50 mL h^{-1} [7,29]. When the flow cell (volume, 0.6 mL) was filled, the pump was stopped and the monitor was used to record the power–time curves of the bacterial growth. The rest of bacterial suspension was discarded. Generally, the experiments were stopped when the second peak came to an end. Data were expressed with their corresponding standard errors and evaluated by the one-way analysis of variance. Then the data were subjected to the least significant difference (LSD) test.

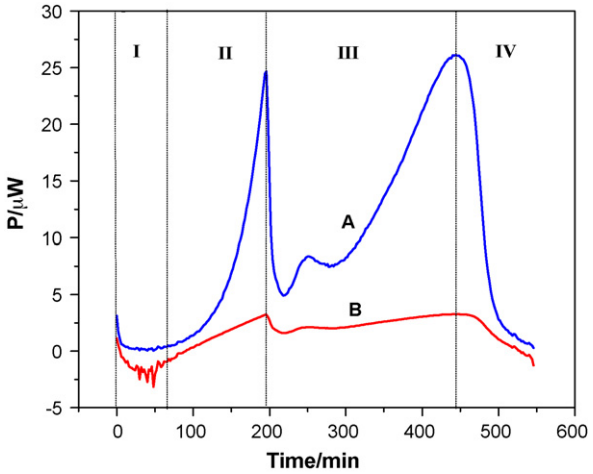

Fig. 1. The power–time curves of *S. aureus*. (A) The growth thermogenic curve of *S. aureus* medium at 37 °C; (B) the fitting logarithmic growth curve of (A). (I) Lag phase; (II) log growth phase; (III) non-log growth phase; (IV) decline phase.

Before tested by Hadamard transform imaging microscope system, the cell suspension of *S. aureus* was added with the MB/TiO_2 nanocomposites suspension and shaked vigorously. Smears for the mixture of suspension were made into slides according to standard cytobiological methods. Double distilled water was used throughout the experiment. After 5-min fixation with cold 90% ethanol, the smears were washed with water three times to remove the ethanol in the cells. Then the slides were washed with water and PBS three times. Glycerin buffer (50%, prepared with PBS) was used as the mounting medium for the slides. The pixel resolution of the HT image is 0.60 μm/pixel when the image is captured with a 25×/0.65 N.A. objective (Fig. SI 1). This valve is close to the resolving power of the microscope ($\delta = 0.50$ μm, calculated according to $\delta = 0.61\lambda$/N.A.). Through the observation with ocular under bright area, the tinct parts are considered as the region of bacteria. The detailed operation process is described in the literatures [30,31].

3. Results and discussion

3.1. The power–time curves of S. aureus

The growth thermogenic curve of bacteria can be classified into four phases, i.e., lag phase, log growth phase, non-log growth phase, and decline phase (Fig. 1). The growth thermogenic curves of *S. aureus* at 37 °C in the absence and presence of different inhibitors at the same concentration of 60 μM are presented (Fig. 2). In the presence of TiO_2, MB and MB/TiO_2 nanocomposites, the growth rate and heat production in log growth phase are both on decrease as compared to those without drugs. However, the shape of the heat production curve remains almost the same at low concentrations of inhibitors except that the time to detection of the first peak becomes longer. 60 μM of TiO_2 makes the maximum power (P_m) declined but the time to detection of the first peak (t_P) remains almost the same. In contrast, the addition of MB and MB/TiO_2 nanocomposites both make the P_m declined and the t_P longer. It can be seen that TiO_2, MB and MB/TiO_2 nanocomposites are all

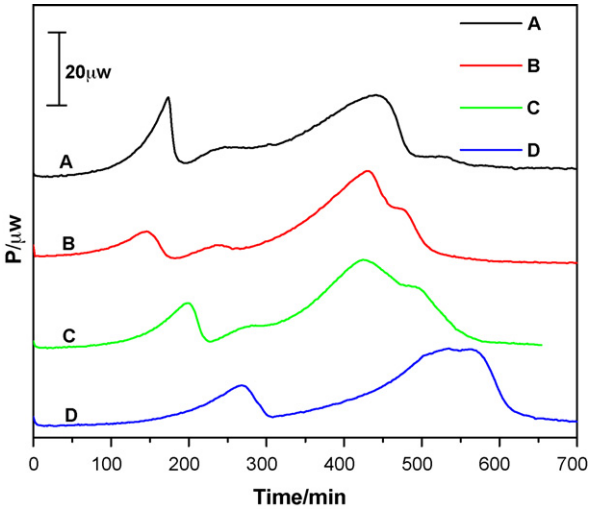

Fig. 2. The power–time curves of *S. aureus* growth in the presence of different chemicals at the same concentration of 60 μM. (A) Control; (B) nano-TiO_2 suspension; (C) MB; (D) MB/TiO_2 nanocomposites suspension.

able to inhibit the log growth metabolism (first peak) of *S. aureus* in the order TiO_2 < MB < MB/TiO_2 nanocomposites. The reason why the inhibitory effect of MB/TiO_2 nanocomposites on *S. aureus* is much greater than that of MB and TiO_2 is probably because MB/TiO_2 nanocomposites have the so-called synergistic effect.

The thermogenic curves of its growth affected by different concentrations of MB/TiO_2 nanocomposites suspension are shown in Fig. 3. From the power–time curves, it can be seen that the shapes of the metabolic thermogenic curves have almost no change at low concentrations of MB/TiO_2 nanocomposites (<40 μM). While at higher concentrations of MB/TiO_2 nanocomposites up to 100 μmol L^{-1}, the first peak disappears and the shapes of total curves have remarkable changes that the lag phase becomes longer. It indicates that MB/TiO_2 nanocomposites have a significant inhibitory effect on *S. aureus* growth.

It can be concluded that with the increase of the concentration of the inhibitor, the lag phase, i.e., the period between the beginning of the test and the ascending phase of the power–time curves, becomes longer and the maximum heat power (P_m) decreases.

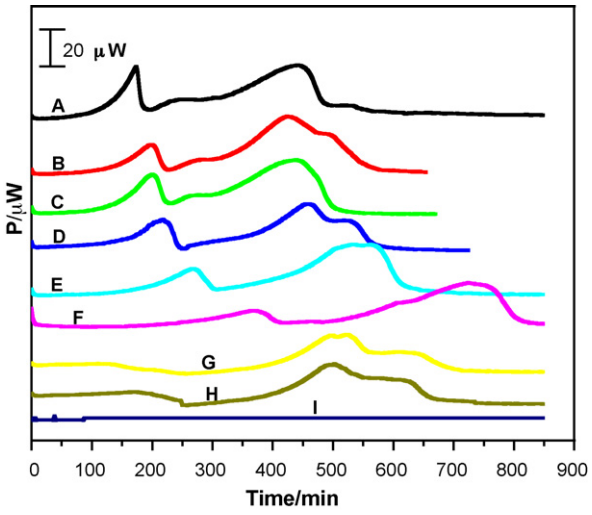

Fig. 3. The power–time curves of *S. aureus* growth in the presence of MB/TiO_2 nanocomposites suspension at different concentrations. (A) control; (B) 8 μM; (C) 20 μM; (D) 40 μM; (E) 60 μM; (F) 80 μM; (G) 100 μM; (H) 150 μM; (I) 200 μM.

3.2. Thermokinetics parameters

As described previously [2], the heat production in the logarithmic growth phase is exponential and can be expressed as follows:

$$P_t = P_0 \exp(kt) \quad (1)$$

or

$$\ln P_t = \ln P_0 + kt \quad (2)$$

where k represents the growth rate constant and P_0 and P_t are the heat production of bacterial growth at the time $t = 0$ and t, respectively. The thermogenic curves of the logarithmic growth phase can be applied by Eqs. (1) and (2). Therefore, the growth rate constant (k) can be obtained by making use of the data $\ln P_t$ and t taken from the curves to fit a linear regression. Based on the growth rate constants at different concentration of an inhibitor, the effect of the inhibitor on the bacterial growth can be quantified.

To describe the activity of MB/TiO_2 nanocomposites on *S. aureus*, the inhibitory ratio (I, %) can be defined as follows:

$$I\ (\%) = \frac{k_0 - k_C}{k_0} \times 100 \quad (3)$$

where k_0 and k_C are the growth rate constant of the control and that in the presence of an inhibitor with a concentration of C, respectively. Through the relationship of I vs. C, we get the half-inhibitory concentration (IC_{50}) for an inhibitor.

The generation time (t_G) can be obtained by the following equation:

$$t_G = \frac{\ln 2}{k} \quad (4)$$

In this work, t_G of the control (25.62 min) agrees well with the value in literature [32].

3.3. Influence of the concentration of MB/TiO_2 nanocomposites on the growth rate constant (k)

The antibacterial effect of MB/TiO_2 nanocomposites is studied through the relationship between growth rate constant (k) and the concentration of inhibitor (C). Table 1 shows that the growth rate constant (k) decreases with the increase in the concentration (C) of MB/TiO_2 nanocomposites. The relationship between the growth rate constant (k) and the corresponding concentration of MB/TiO_2 nanocomposites can be thus established as a linear regression as follows:

$$k = 0.02655 - 1.47817 \times 10^{-4} C, \quad R^2 = 0.95 \quad (5)$$

3.4. Influence of the concentration of MB/TiO_2 nanocomposites on the maximum heat power (P_m)

The maximum heat power of growth phase (P_m) is an important parameter to the metabolism of microbes as it represents the ability of microbes to grow at specific conditions. Increasing concentrations of MB/TiO_2 nanocomposites make P_m declined dramatically when the concentration is above 100 μM. This result is in accordance with the relationship between k and C.

3.5. Relationship between the inhibitory ratios, half-inhibitory concentration, generation time and the concentration of MB/TiO_2 nanocomposites

The half-inhibitory concentration (IC_{50}) is widely used to evaluate the sensitivity of bacteria to inhibitors. The inhibitory ratios (I) at the corresponding concentration of MB/TiO_2 nanocomposites (C) can be calculated by Eq. (3). Then the I is fitted linearly with the

Table 1
Parameters of *S. aureus* growth with different concentrations of MB/TiO_2 nanocomposites at 37.0 °C.

C (μmol L^{-1})	P_m (μW)	k (min^{-1})	R^a	SD[b]	t_G (min)	I (%)	IC_{50} (μmol L^{-1})
0	28.76	0.0275	0.9998	0.0116	25.62	0	89.53
8	28.62	0.0257	0.9987	0.0124	26.64	10.67	
20	28.42	0.0247	0.9989	0.0271	28.06	12.69	
40	27.83	0.0191	0.9985	0.0343	36.2	28.2	
60	26.80	0.0195	0.9983	0.0184	47.64	43.22	
80	25.95	0.0118	0.9986	0.0135	57.12	45.45	
100	23.69	0.0104	0.9987	0.0172	66.12	59.24	
150	13.06	0.0063	0.9747	0.00188	134.6	78.53	
200	–	–	–	–	–	100	

[a] R is the correlation coefficient.
[b] SD is the standard deviation.

C as is shown in Fig. 4 and the equation can be expressed as linear regression:

$$I = 6.37613 + 0.48726C, \quad R^2 = 0.99 \tag{6}$$

When $I = 50$, $IC_{50} = 89.53$ μmol L^{-1}.

The generation time (t_G) increases remarkably with the increase in MB/TiO_2 nanocomposites concentration (C) above 100 μM (Table 1).

In order to compare the effect of inhibition, a function of the maximum heat power (P_m) on the time to detection of the first peak (t_P) is shown for direct description (Fig. 5). In this figure, the peak power (P_m) decreases while the time to detection of this peak increases when the concentration of MB/TiO_2 nanocomposites increases (<100 μM). Leib and co-workers used calorimetry to make the detection times of <4 h for *S. pneumonide* and *N. meningitides* and <10 h for *Listeria monocytogenes* using as little as 10 μL of cerebrospinal fluid [33]. It proved calorimetry a new rapid and accurate diagnostic method for detection of bacterial meningitis from a small volume of cerebrospinal fluid. The concept "time to detection" can be a good approach to directly evaluate the inhibitory effect in many fields.

3.6. Mechanism of cell damage of *S. aureus* exposed to MB/TiO_2 nanocomposites

Drug-resistant gram-positive bacteria such as *S. aureus* have already been identified as the major public health problems [34]. However, the mechanism of cell damage of *S. aureus* incubated with MB/TiO_2 nanocomposites is not reported thus far. In this work, transmission emission microscopy (TEM, Fig. SI 1A–D) as well as Hadamard transform imaging microscopy (HT, Fig. SI 1E–H) addresses the mechanism of interaction of MB/TiO_2 nanocomposites with gram-positive bacteria.

In Fig. SI 1A and B (with TiO_2), the cells are intact but become broken when incubated with MB (Fig. SI 1C). In Fig. SI 1D (with MB/TiO_2), the single cell has several interacting sites on the cell membrane (red arrows). According to the mechanism of inhibition and the data obtained, it reveals that the bacterial cell has multiple sites of cell division [35]. The MB/TiO_2 nanocomposites trigger this action on several sites. Most probably, the free radicals generated at the surface of MB/TiO_2 nanocomposites interact with the membrane phospholipids of bacterial cell and thus induce destruction of cells. The presence of MB/TiO_2 nanocomposites can induce modification in membrane permeability which promotes cell death [36]. The cell membrane appears to have been considerably damaged and its integrity is largely destroyed. It can be seen from the transmission microscopic images that the MB/TiO_2 nanocomposites cause much more serious damage to the bacteria than MB and TiO_2 alone, which is consistent with the microcalorimetric evaluation. In addition, some MB/TiO_2 particles have entered into the cell to make it swollen (Fig. SI 1D, blue arrows).

Due to the higher sensitivity originated from the low background of HT imaging microscopy, it can be used to measure cellular substances more accurately than a common CCD camera [37]. In Fig. SI 1E and F, the cells are not clear as they are not stained because the staining dye can interfere with the signal formed by the fluorescence of MB. Since MB is present in Fig. SI 1G (with MB) and 1H (with MB/TiO_2), a lot of cells can be observed with different degrees of swelling roughly in the order "cells incubated with MB" < "cells incubated with MB/TiO_2" (black circles). Furthermore,

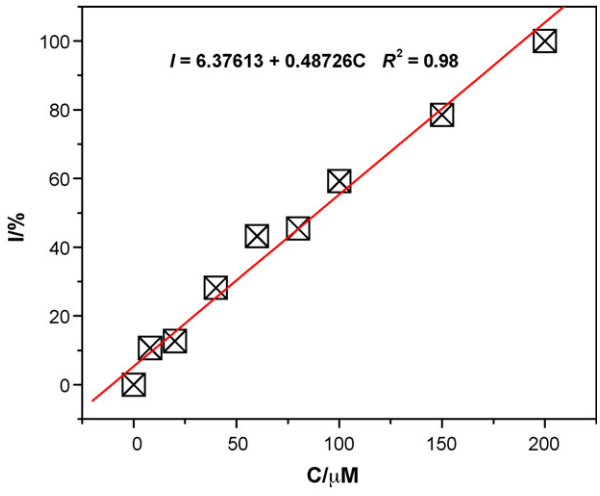

Fig. 4. Relationship between inhibitory ratio and concentration of MB/TiO_2 nanocomposites.

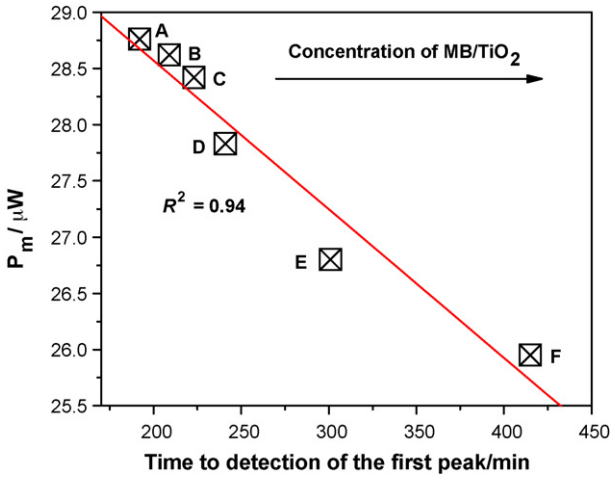

Fig. 5. Relationship between the maximum heat power (P_m) and the time to detection of the first peak (t_P). Concentration of MB/TiO_2 nanocomposites: (A) 0 μM; (B) 8 μM; (C) 20 μM; (D) 40 μM; (E) 60 μM; (F) 80 μM.

some decomposed cells with leaked cytoplasm form aggregates like mini-vesicles and intracellular vacuoles (dashed squares in Fig. SI 1H). The fact that the cell membrane is severely decomposed (Fig. SI 1H) supports the idea that initial interaction takes place on the cell membrane [38]. Damage on cell membrane will lead to the perturbation of various cellular processes, then the leakage of the cytoplasm and finally bacteria inactivation and death [21]. This investigation reveals a number of membrane fragments following the complete destruction of the microbial cell.

In short, the mechanism of cell damage may follow two processes: (1) the nanoparticles interact with several sites on the cell membrane and this interaction may lead to the damage of cell membrane and thereafter the leakage of cytoplasm; (2) the nanoparticles can be passively absorbed into the cell to make the cell swollen and interact with the subcellular organ to inactivate the cell.

4. Conclusions

In conclusion, this work demonstrates microcalorimetry can provide a very good way to study the antibacterial effect of nanocomposites which can not be obtained by conventional bacteriological techniques. It also provides an analytical tool for studying the interaction between cells with nanomaterials since it is crucial to address the challenges of nanobiotechnology. This work provides a new platform for effective design and extensive application of dyes-TiO_2 nanocomposites as an antibacterial, virus-killing, detoxifying and self-cleaning agent in pollution control.

Acknowledgments

We gratefully acknowledge financial support from the National Natural Science Foundation of China (20873096, 20621502 and 20921062), Key Laboratory of Catalysis and Materials Science of Hubei Province and the 973 program from the Ministry of Science and Technology of the People's Republic of China (2009CB939705).

Appendix A. Supplementary data

Supplementary data associated with this article can be found, in the online version, at doi:10.1016/j.tca.2009.12.015.

References

[1] C.N. Yan, Y. Liu, T.Z. Wang, Z.Q. Tan, S.S. Qu, P. Shen, Chemosphere 38 (1999) 891–898.
[2] C.L. Xie, H.K. Tang, Z.H. Song, S.S. Qu, Y.T. Liao, H.S. Liu, Thermochim. Acta 123 (1988) 33–41.
[3] X.J. Xu, Y. Liu, Biol. Trace Elem. Res. 125 (2008) 185–192.
[4] X. Li, Y. Liu, R.M. Zhao, J. Wu, X.S. Shen, S.S. Qu, Biol. Trace Elem. Res. 75 (2000) 167–1755.
[5] X. Li, Y. Liu, J. Wu, H.G. Liang, S.S. Qu, Thermochim. Acta 387 (2002) 57–61.
[6] Y. Yang, J.C. Zhu, Y. Liu, P. Shen, S.S. Qu, J. Biochem. Biophys. Methods 62 (2005) 183–189.
[7] C.L. Xie, G.D. Xu, S.S. Qu, Acta Phys. Chim. Sin. 2 (1986) 363–370.
[8] D.C. Carter, X.M. He, Science 249 (1990) 302–303.
[9] M.I. Simon, H. van Vunakis, J. Mol. Biol. 4 (1962) 488–499.
[10] Y.J. Hu, Y. Liu, R.M. Zhao, J.X. Dong, S.S. Qu, J. Photochem. Photobiol. A: Chem. 179 (2006) 324–329.
[11] S.C. Souza, J.C. Junqueira, Balducci, C.Y. Koga-Ito, E. Munin, A.O.C. Jorge, J. Photochem. Photobiol. B 83 (2006) 34–38.
[12] Y.X. Chen, M.V. Metz, L.T. Li, J. Am. Chem. Soc. 120 (1998) 6374–6379.
[13] S. Horikoshi, et al., Chem. Phys. Lett. 470 (2009) 304–307.
[14] C. Yogi, K. Kojima, et al., J. Mater. Sci. 44 (2009) 821–827.
[15] D. Gutiérrez-Tauste, X. Domènech, N. Casañ-Pastor, J.A. Ayllón, J. Photochem. Photobiol. A: Chem. 187 (2007) 45–52.
[16] A. Franco, et al., J. Hazard. Mater. 161 (2009) 545–550.
[17] J.C. Zhao, T.X. Wu, K.Q. Wu, K. Oikawa, H. Hidaka, N. Serpone, Environ. Sci. Technol. 32 (1998) 2394–2400.
[18] J. Lonnen, S. Kilvington, S. Kehoe, F. Al-Touati, K.G. McGuigan, Water Res. 3 (2005) 877–883.
[19] C. Guillard, T.H. Bui, C. Felix, V. Moules, B. Lina, P. Lejeune, C. R. Chim. 11 (2008) 107–113.
[20] X. Sang, T.G. Phan, S. Sugihara, F. Yagyu, S. Okitsu, N. Maneekarn, W.E.G. Müller, H. Ushijima, Clin. Lab. 53 (2007) 413–421.
[21] Z.X. Lu, L. Zhou, Z.L. Zhang, W.L. Shi, Z.X. Xie, H.Y. Xie, D.W. Pang, P. Shen, Langmuir 19 (2003) 8765–8768.
[22] T. Matsunaga, M. Okochi, Environ. Sci. Technol. 29 (1995) 501–505.
[23] J.C. Ireland, P. Klostermann, E.W. Rice, R.M. Clark, Appl. Environ. Microbiol. 59 (1993) 1668–1670.
[24] S. Koide, T. Nonami, Food Control 18 (2007) 1121–1125.
[25] D.M. Blake, P.C. Maness, Z. Huang, E.J. Wolfrum, Sep. Purif. Methods 281 (1999) 1–50.
[26] J.W. Seo, H. Chung, M.Y. Kim, J. Lee, I.H. Choi, Small 3 (2007) 850–853.
[27] T. Ashikaga, M. Wada, H. Kobayashi, M. Mori, Y. Katsumura, H. Fukui, S. Kato, M. Yamaguchi, T. Takamatsu, Mutat. Res. 466 (2000) 1–7.
[28] B. Valeur, J.C. Brochon, Special Issue: Sixth International Conference on Methods and Applications of Fluorescence Spectroscopy, Paris, France, September 12–15, 1999.
[29] X. Li, Y. Liu, J. Wu, S.S. Qu, Thermochim. Acta 375 (2001) 109–113.
[30] H.W. Tang, M.N. Luo, Y.P. Xiong, G.Q. Chen, Anal. Bioanal. Chem. 381 (2005) 901–906.
[31] H.W. Tang, G.Q. Chen, J.S. Zhou, Q.S. Wu, Anal. Chim. Acta 468 (2002) 27–34.
[32] S.R. Tatini, S.A. Stein, H.M. Soo, J. Food Sci. 41 (1976) 133–135.
[33] A. Trampuz, A. Steinhuber, M. Wittwer, S.L. Leib, BMC Infect. Dis. 7 (2007) 116–121.
[34] B.R. Lyon, R.A. Skurray, Microbiol. Rev. 51 (1987) 88–134.
[35] P. Amézaga-Madridetal, R. Silveyra-Morales, L. Córdoba-Fierro, G.V. Nevárez-Moorillon, M. Miki-Yoshida, E. Orrantia-Borunda, F.J. Solis, J. Photochem. Photobiol. B: Biol. 70 (2003) 45–50.
[36] C. Văcăroiu, M. Enache, M. Gartner, G. Popescu, M. Anastasescu, A. Brezeanu, N. Todorova, T. Giannakopoulou, C. Trapalis, L. Dumitru, World J. Microbiol. Biotechnol. 25 (2009) 27–31.
[37] H.W. Tang, M.N. Luo, T. Li, P. Li, Anal. Sci. 22 (2006) 701–706.
[38] B. Halliwell, J. Lonnen, M.C. Gutteridge, Free Radicals in Biology and Medicine, Oxford University Press, New York, 1989, pp. 86–97.